Journal of Scientific Computing manuscript No.
(will be inserted by the editor)

A robust randomized indicator method for accurate symmetric eigenvalue detection

Zhongyuan Chen · **Jiguang Sun** · **Jianlin Xia**

Received: date / Accepted: date

Abstract We propose a robust randomized indicator method for the reliable detection of eigenvalue existence within an interval for symmetric matrices A. An indicator tells the eigenvalue existence based on some statistical norm estimators for a spectral projector. Previous work on eigenvalue indicators relies on a threshold which is empirically chosen, thus often resulting in under or over detection. In this paper, we use rigorous statistical analysis to guide the design of a robust indicator. Multiple randomized estimators for a contour integral operator in terms of A are analyzed. In particular, when A has eigenvalues inside a given interval, we show that the failure probability (for the estimators to return very small estimates) is extremely low. This enables to design a robust rejection indicator based on the control of the failure probability. We also give a prototype framework to illustrate how the indicator method may be applied numerically for eigenvalue detection and may potentially serve as a new way to design randomized symmetric eigenvalue solvers. Unlike previous indicator methods that only detect eigenvalue existence, the framework also provides a way to find eigenvectors with little extra cost by reusing computations from indicator evaluations. Extensive numerical tests show the reliability of the eigenvalue detection in multiple aspects.

Keywords Symmetric matrices · Eigenvalue indicator · Randomized estimator · Statistical analysis · Failure probability · Shifted linear systems

Mathematics Subject Classification (2010) 65F15, 65F30, 68W20

1 Introduction

In scientific computing and practical applications, it often needs to find selected interior eigenvalues for large matrices. Examples include transmission eigenvalue problems arising from inverse scattering, linear response eigenvalue problems in quantum chemistry, and interior eigenvalue problems in density-functional theory. In this paper, we consider a randomized strategy for reliably detecting the existence of (interior) eigenvalues of a real symmetric matrix A within target intervals. The discussions can also be extended to some generalized eigenvalue problems.

In matrix computations, randomization has been widely used in solving linear systems and in finding low-rank approximations. On the other hand, the development of randomized eigenvalue methods is relatively limited. (Selected recent work may be found in [6,26,38].) Recently, a type of *indicator* eigensolvers is proposed in [17–19] that use randomized detection of eigenvalues. Suppose A has k eigenvalues inside an interval (a,b) on the real axis that is circumscribed by a Jordan curve $\mathscr{C}$. Let $\mathbf{i}=\sqrt{-1}$ and

$$P=\frac{1}{2\pi\mathbf{i}}\int_{\mathscr{C}}(sI-A)^{-1}ds, \tag{1}$$

Z. Chen
Division of Biostatistics, Medical College of Wisconsin, Milwaukee, WI 53223, USA
E-mail: zhchen@mcw.edu

J. Sun
Department of Mathematical Sciences, Michigan Technological University, Houghton, MI 49931, USA
E-mail: jiguangs@mtu.edu

J. Xia
Department of Mathematics, Purdue University, West Lafayette, IN 47907, USA
E-mail: xiaj@purdue.edu

which is a projection matrix. It is known that $\|P\|_2 = 1$ if $k \geq 1$ or $\|P\|_2 = 0$ if $k = 0$ (see (4) below). The indicator methods in [17–19] thus try to estimate $\|P\|_2$ based on $\|Pz\|_2$ with a random vector z. If there are eigenvalues inside, the region is repeatedly partitioned and checked.

Like various existing contour-integral eigensolvers in [2,23,29,33,47] and also eigensolvers based on rational approximations [4,20,43], such indicator eigensolvers are very attractive for finding interior eigenvalues because of their scalability. They also enjoy two additional significant features: the simplicity and the convenient error control. The indicator eigensolvers do not need to extract eigenspace information corresponding to the k eigenvalues and do not need to estimate k. They only apply P to one single random vector z instead of about k (and often more) random vectors [29,33,36]. These indicator eigensolvers can also conveniently control the accuracy since they use a domain refinement process to decide the convergence instead of, say, Rayleigh-Ritz iterations or Krylov subspace iterations.

An intuitive indicator is based on the following norm:

$$\xi = \|Pz\|_2. \tag{2}$$

With appropriate choices of z, ξ may be viewed as an estimator for $\|P\|_2$. Thus, if ξ is larger than a certain threshold ε, then the region is *accepted* (considered to have eigenvalues inside). The reliability of the indicator in (2) is unclear in previous work, so other variations are tried. One is in [17] based on a power method that is more reliable but is not practical due to its high expense in general. Another indicator is designed in [18] based on the ratio of two quadrature approximations to $\|Pz\|_2$. Let y_m be the m-point quadrature approximation to $\|Pz\|_2$. (A specific form of y_m can be found in (22) later.) With a threshold δ, the region is *rejected* (claimed to have no eigenvalue inside) if

$$y_{2m}/y_m < \delta. \tag{3}$$

Despite all the attractive features, all such indicator methods have one key limitation. That is, the choice of the thresholds to determine the existence of eigenvalues is fully based on heuristics. For example, a rejection threshold $\varepsilon = 0.1$ is used for (2) in [17]. In [18], a rejection threshold $\delta = 0.2$ is used for (3), and later in [19], $\delta = 0.05$ is used. All these thresholds are empirical choices based on numerical trials without justification of their reliability. Such thresholds around 0.1 are sensitive for making the $0/1$ decision. If a large threshold is used, an interval may be incorrectly rejected so as to miss eigenvalues. If a small threshold is used, many intervals without eigenvalues may be accepted. This would bring extra costs and even produce "*spurious* eigenvalues" which are often near the true eigenvalues but may also be farther away.

Thus, it is difficult to control the quality of the previous indicators. In particular, all the previous work lacks the ability to correctly reject an interval with high confidence. In addition, previous indicator-based eigenvalue methods in [17–19] can only be used to find the eigenvalues and miss a way to conveniently extract eigenvector information.

Therefore in this work, we aim to design robust eigenvalue indicators based on rigorous statistical analysis of different types of randomized estimators. We also give a way to compute eigenvectors for the identified eigenvalues with very little extra cost. The main significance includes the following.

- Rigorous statistical analysis is provided as guidelines for indicator designs. Based on different properties of the projector P and different options of the random vector z, we consider multiple randomized estimators and provide refined expectation and variance results and, moreover, tight failure probability bounds. With the existence of eigenvalues, at least one estimator has reasonably small *failure probability*, even with only one random vector z. We also show that a larger number of eigenvalues in an interval leads to even more reliable estimates.
- Guided by the analysis, we design a robust rejection indicator. We control the rejection reliability through the control of failure probabilities. Our probability analysis indicates that, if an interval contains eigenvalues, the probability for some estimators to return estimates smaller than a tiny threshold ε (such as 10^{-15}) is extremely low. If a certain estimate is indeed smaller than ε, then the interval can be rejected with high confidence.
- Unlike the methods in [17–19] that rely on a single threshold to accept/reject an interval, here we give a combination of multiple indicators so as to provide highly confident acceptance/rejection decisions.
- We then lay out a prototype framework to illustrate how our indicator method may be applied numerically for eigenvalue detection and may potentially be useful and for finding eigenvalues accurately. In a bisection scheme, the indicators are quickly evaluated via preconditioned Lanczos iterations for *partially* solving multiple shifted linear systems, where Krylov subspace information is reused to rapidly evaluate relevant vector norms without explicit linear solutions.
- We can further produce the eigenvectors with little extra cost by reusing computations that are already available from the indicator evaluations. The new indicator method can also be extended to some symmetric generalized eigenvalue problems.

The work then gives a potentially practical option to extend randomization to the design of eigenvalue methods. We point out that the prototype eigenvalue algorithm presented in this work is only an illustration of how randomized indicator methods may be made reliable for designing eigensolvers. Our purpose is *not* to present a fully practical eigensolver that can already compete with many existing well-designed eigensolvers. The practical eigenvalue solution will be considered in subsequent work. Nevertheless, several numerical tests indicate that our robust indicator strategy can nicely capture the eigenvalues and reach a prespecified accuracy. In comparison, the original indicator strategy from [18,19] with various threshold choices often produces spurious eigenvalues and sometimes misses eigenvalues.

The design of the robust rejection indicator is given in Section 2. Section 3 presents a framework for numerically applying the indicator method to eigenvalue detection and solution, followed by some numerical experiments in Section 4 and some conclusions in Section 5. In the paper, $z \sim \mathcal{N}(0, I_n)$ means a vector z is a length-n standard Gaussian random column vector and $z \sim \mathcal{U}(S_{n-1})$ means z is uniformly and randomly selected from the unit n-sphere S_{n-1}. Also, diag() denotes a diagonal matrix and trace() denotes the trace of a matrix.

2 Design of robust randomized eigenvalue indicators

Suppose the symmetric matrix A is $n \times n$ and has an eigenvalue decomposition

$$A = Q\Lambda Q^T,$$

where Q is orthogonal and $\Lambda = \mathrm{diag}(\lambda_1, \ldots, \lambda_n)$ is for the eigenvalues $\lambda_1, \ldots, \lambda_n$. For convenience, we suppose $\lambda_1, \ldots, \lambda_k \in (a,b)$ (enclosed by $\mathscr{C}$) are the desired eigenvalues. Then Cauchy's residual theorem yields that P in (1) can be written as

$$P = Q\left(\frac{1}{2\pi \mathbf{i}} \int_{\mathscr{C}} (sI - \Lambda)^{-1} ds\right) Q^T = Q\,\mathrm{diag}(I_k, 0) Q^T, \tag{4}$$

where I_k is the $k \times k$ identity matrix. Accordingly, we have

$$\|P\|_2 = 1, \quad \|P\|_F = \sqrt{k}, \quad \mathrm{trace}(P) = k. \tag{5}$$

To support our design of robust indicators, we consider some randomized estimators like in (2) so as to probe the properties of P like in (5). The estimators are based on Pz with a single appropriately chosen random vector z. It is well known that randomized methods may be used for norm and trace estimations. There have been extensive studies of the performance of these estimators. See [5,9,14,21,42] for some earlier work and [7,25,32] for examples of more recent studies. Also see [10,16,24] for some reviews. Here, the special form of P enables us to perform more concrete studies of the behaviors of several types of randomized estimators. We would like to show how such estimators can be used to confidently decide the existence of eigenvalues inside the interval (a,b).

2.1 Analysis of randomized estimators for P

We first look at different types of estimators for statistically extracting information on the projector P. Following the properties of P, our studies below provide some refined results on the expectation, variance, and probability. We would like to point out two things.

- For the probability studies when there are eigenvalues inside the interval, our goal is *not* to show how close the randomized estimates are to the exact norms or traces. Instead, we would like to show that, with high probability, the estimates are not too small. In other words, the *failure probability* or the probability $\Pr(\xi \le \varepsilon)$ for an estimator ξ with small ε is very low, even with just one vector z. For some estimators ξ, we can make $\Pr(\xi \le \varepsilon)$ go to 0 as $\varepsilon \to 0$. In contrast, traditional studies of the failure probabilities for norm and trace estimators are typically more conservative since they would require many more random vectors to reach small failure probabilities.
- Some of the estimators below are related. However, we use different strategies to analyze them so as to obtain results that behave differently for different parameters.

One common way is to consider $\|Pz\|_2$ as an estimator of $\|P\|_2$ like in [9,42]. Here with the form of P in (4), we have the following result.

Theorem 1 *Suppose there are $k \ge 1$ eigenvalues in the interval enclosed by $\mathscr{C}$. Let $z \sim \mathcal{U}(S_{n-1})$ and $\xi_U^{(1)} = \|Pz\|_2$. Then for $0 < \varepsilon < 1$,*

$$\sqrt{\frac{k-1}{n}} < \mathrm{E}(\xi_U^{(1)}) \le \sqrt{\frac{k}{n}}, \quad \mathrm{Var}(\xi_U^{(1)}) < \frac{1}{n}, \quad \Pr(\xi_U^{(1)} \le \varepsilon) \le \varepsilon\sqrt{\frac{2n}{\pi}}.$$

Proof From (4), we have

$$(\xi_U^{(1)})^2 = \|Q\,\mathrm{diag}(I_k,0)Q^T z\|_2^2 = \|\tilde{z}_{1:k}\|_2^2, \tag{6}$$

where $\tilde{z}_{1:k}$ is the vector given by the first k entries of $\tilde{z} = Q^T z$. It is obvious that $\tilde{z} \sim \mathscr{U}(S_{n-1})$. Since $\|\tilde{z}_{1:k}\|_2^2$ follows a beta distribution with parameters $(\frac{k}{2}, \frac{n-k}{2})$ [1], $\mathrm{E}((\xi_U^{(1)})^2) = \frac{k}{n}$. According to Jensen's inequality, $\mathrm{E}(\xi_U^{(1)}) \le \sqrt{\frac{k}{n}}$. Also, $\xi_U^{(1)}$ has probability density function $\frac{t^{k/2-1}(1-t)^{(n-k)/2-1}}{\mathscr{B}(k/2,(n-k)/2)}$, where $\mathscr{B}(s,t)$ is the beta function. Let $\Gamma(t)$ be the gamma function. Then the standard expectation computation yields

$$\mathrm{E}(\xi_U^{(1)}) = \frac{1}{\mathscr{B}(k/2,(n-k)/2)}\int_0^1 t^{1/2}t^{k/2-1}(1-t)^{(n-k)/2-1}dt = \frac{\Gamma((k+1)/2)}{\Gamma(k/2)}\frac{\Gamma(n/2)}{\Gamma((n+1)/2)}.$$

Standard properties of the gamma function yield (specifically, from inequalities by Gautschi [12] and Wendel [40], respectively)

$$\frac{\Gamma((k+1)/2)}{\Gamma(k/2)} > \sqrt{\frac{k-1}{2}}, \quad \frac{\Gamma((n+1)/2)}{\Gamma(n/2)} \le \sqrt{\frac{n}{2}}. \tag{7}$$

Thus, $\mathrm{E}(\xi_U^{(1)}) > \sqrt{\frac{k-1}{n}}$. Also,

$$\mathrm{Var}(\xi_U^{(1)}) = \mathrm{E}((\xi_U^{(1)})^2) - (\mathrm{E}(\xi_U^{(1)}))^2 < \frac{k}{n} - \frac{k-1}{n} = \frac{1}{n}.$$

Finally, the probability bound can be obtained from [9, proof for Theorem 1] since P is positive semidefinite and $\|P\|_2 = 1$. □

Another way to study the behaviors of the estimator $\xi_U^{(1)}$ is in terms of vector norm estimation as follows. In the next subsection, we will see that this yields some bounds of different qualities.

Theorem 2 *With the same conditions as in Theorem 1, we have*

$$\mathrm{E}(\xi_U^{(1)}) \ge \sqrt{k}\omega_n, \quad \mathrm{Var}(\xi_U^{(1)}) \le \frac{k}{n} - k\omega_n^2, \quad \Pr(\xi_U^{(1)} \le \varepsilon) \le \frac{2\varepsilon}{\pi\omega_n},$$

where ω_n is the Wallis factor [21]: $\omega_n = \begin{cases} \frac{(n-2)!!}{(n-1)!!}, & \text{if } n \text{ is odd,} \\ \frac{2}{\pi}\frac{(n-2)!!}{(n-1)!!}, & \text{otherwise.} \end{cases}$

Proof Let q_i be the unit eigenvector corresponding the eigenvalue λ_i, $i = 1,\ldots,k$. From (4) and the Cauchy-Schwarz inequality, we have

$$\|Pz\|_2 = \|\,\mathrm{diag}(I_k,0)Q^T z\|_2 = \sqrt{\sum_{i=1}^k (q_i^T z)^2} \ge \frac{1}{\sqrt{k}}\sum_{i=1}^k |q_i^T z|.$$

According to [21], $\mathrm{E}(\frac{|q_i^T z|}{\omega_n}) = \|q_i\|_2$. Note $\|q_i\|_2 = 1$. Then

$$\mathrm{E}(\xi_U^{(1)}) \ge \frac{1}{\sqrt{k}}\sum_{i=1}^k \mathrm{E}(|q_i^T z|) = \frac{1}{\sqrt{k}}\omega_n\sum_{i=1}^k \|q_i\|_2 = \sqrt{k}\omega_n.$$

The variance satisfies $\mathrm{Var}(\xi_U^{(1)}) = \mathrm{E}((\xi_U^{(1)})^2) - (\mathrm{E}(\xi_U^{(1)}))^2 \le \frac{k}{n} - k\omega_n^2$. Also, $\|Pz\|_2 \ge |q_1^T z|$ yields

$$\Pr(\xi_U^{(1)} \le \varepsilon) \le \Pr(|q_1^T z| \le \varepsilon) = \Pr(\frac{|q_1^T z|}{\omega_n} \le \frac{\varepsilon}{\omega_n}) \le \frac{2\varepsilon}{\pi\omega_n},$$

where the last inequality is based on [21, Theorem 2.4]. □

In the previous two theorems, the probability bounds do not depend on k. To study the impact of k on the probability, we show another result that gives smaller probability bounds for larger k. It is based on the estimation of $\|P\|_F^2 = k$.

Theorem 3 *Suppose there are $k \ge 1$ eigenvalues in the interval enclosed by $\mathscr{C}$ and $k+1 < n$. Let $z \sim \mathscr{U}(S_{n-1})$ and $\xi_U^{(2)} = \|Pz\|_2^2$. Then for $0 < \varepsilon < 1$,*

$$\mathrm{E}(\xi_U^{(2)}) = \frac{k}{n}, \quad \mathrm{Var}(\xi_U^{(2)}) = \frac{2k(n-k)}{n^2(n+2)}, \quad \Pr(\xi_U^{(2)} \le \varepsilon) < \sqrt{\frac{2}{k\pi}}\,(\varepsilon(n+1-k))^{k/2}.$$

Proof The expectation has been mentioned in the proof of Theorem 1. Another way to understand this is to view $n\xi_U^{(2)} = n\|Pz\|_2^2$ as an unbiased estimator for $\|P\|_F^2$ [14]. To show the variance, we use a result in [14, Lemma 2.2] and the fact that all the nonzero singular value of P are equal to 1 to get

$$\mathrm{Var}(n\xi_U^{(2)}) = \frac{2}{n+2}(nk - \|P\|_F^4) = \frac{2k(n-k)}{n+2}.$$

Following (6) in the proof of Theorem 1, we have

$$\Pr(\xi_U^{(2)} \le \varepsilon) = \Pr(\|\tilde{z}_{1:k}\|_2^2 \le \varepsilon) = \frac{1}{\mathscr{B}(k/2,(n-k)/2)} \int_0^\varepsilon t^{k/2-1}(1-t)^{(n-k)/2-1} dt.$$

For the purpose of deriving a tight bound for this, let

$$c_{k,n} = \frac{1}{\mathscr{B}(k/2,(n-k)/2)}, \quad \beta_{k,n} = \sqrt{\frac{k}{2\pi}}\,(n+1-k)^{k/2}.$$

In the following, we show $c_{k,n} < \beta_{k,n}$ for all $k \ge 1$. If $k = 1$, it is shown in [9] that $c_{1,n} < \sqrt{\frac{n}{2\pi}} = \beta_{1,n}$. If $k = 2$, $c_{2,n} = \Gamma(\frac{n}{2})/\Gamma\left(\frac{n}{2}-1\right) = \frac{n}{2}-1$. Since it always holds that $\frac{n}{2}-1 < \sqrt{\frac{1}{\pi}}\,(n-1) = \beta_{2,n}$, we have $c_{2,n} < \beta_{2,n}$. If $k > 2$, we show the bound as follows. With given k, the asymptotic behavior of the gamma function as $n \to \infty$ yields

$$c_{k,n} = \frac{\Gamma(\frac{n}{2})}{\Gamma\left(\frac{k}{2}\right)\Gamma\left(\frac{n-k}{2}\right)} \sim \frac{\left(\frac{n-k}{2}\right)^{k/2}}{\Gamma\left(\frac{k}{2}\right)} = \frac{(n-k)^{k/2}}{2^{k/2}\Gamma\left(\frac{k}{2}\right)}.$$

Now consider $g_n \equiv \frac{c_{k,n}}{(n-k)^{k/2}}$. Notice that

$$g_n > g_{n+2},$$

which is equivalent to $\left(\frac{n+2-k}{n-k}\right)^{k/2} > \frac{c_{k,n+2}}{c_{k,n}} = \frac{n}{n-k}$. (Note $\Gamma(\frac{n}{2}+1) = \frac{n}{2}\Gamma(\frac{n}{2})$.) This inequality holds since $\left(1+\frac{2}{n-k}\right)^{k/2} > 1 + \frac{k}{n-k}$ for $k > 2$, which follows from the (generalized) binomial expansion. Thus, the sequences $\{g_{2j-1}\}$ and $\{g_{2j}\}$ strictly monotonically decrease with j. Note $n > k+1$. Then

$$g_n \le \max\{g_{k+1}, g_{k+2}\} = \max\left\{\frac{\Gamma(\frac{k+1}{2})}{\Gamma\left(\frac{k}{2}\right)\Gamma\left(\frac{1}{2}\right)}, \frac{\Gamma(\frac{k+2}{2})}{2^{k/2}\Gamma\left(\frac{k}{2}\right)}\right\} = \frac{\Gamma(\frac{k+1}{2})}{\Gamma\left(\frac{k}{2}\right)\sqrt{\pi}} \le \sqrt{\frac{k}{2\pi}},$$

where the last inequality follows from Wendel's inequality like in (7). Thus,

$$c_{k,n} \le \sqrt{\frac{k}{2\pi}}\,(n-k)^{k/2} < \beta_{k,n}.$$

Combining the results to get $c_{k,n} < \beta_{k,n}$ for all $1 \le k < n$. Accordingly, with $k+1 < n$, we have

$$\begin{aligned}\Pr(\xi_U^{(2)} \le \varepsilon) &< \beta_{k,n}\int_0^\varepsilon t^{k/2-1}(1-t)^{(n-k)/2-1}dt < \beta_{k,n}\int_0^\varepsilon t^{k/2-1}dt = \frac{2\varepsilon^{k/2}\beta_{k,n}}{k} \\ &= \frac{2\varepsilon^{k/2}}{k}\sqrt{\frac{k}{2\pi}}\,(n+1-k)^{k/2} = \sqrt{\frac{2}{k\pi}}\,(\varepsilon(n+1-k))^{k/2}.\end{aligned}$$

□

Note that the condition $k+1 < n$ in the theorem is merely for the convenience of proving the probability bound. When $k = n$, the probability bound is trivially true since $\xi_U^{(2)} \equiv 1$ and $\Pr(\xi_U^{(2)} \le \varepsilon) = 0$. When $k = n-1$, as long as n is not too small, the probability bound also holds.

Other than the estimation of the norms as above, we may also consider the estimation of $\mathrm{trace}(P)$ with another choice of z. The following theorem is based on some results on the χ^2 distribution.

Theorem 4 *Suppose there are $k \ge 1$ eigenvalues in the interval enclosed by $\mathscr{C}$. Let $z \sim \mathscr{N}(0, I_n)$ and $\xi_N^{(2)} = \|Pz\|_2^2$. Then for $0 < \varepsilon < 1$,*

$$\mathrm{E}(\xi_N^{(2)}) = k, \quad \mathrm{Var}(\xi_N^{(2)}) = 2k, \quad \Pr(\xi_N^{(2)} \le \varepsilon) \le \sqrt{1 - \exp(-\frac{2}{\pi}\varepsilon)}.$$

Proof For $z \sim \mathcal{N}(0, I_n)$, $\xi_N^{(2)} = z^T P^2 z = z^T P z$ is actually an unbiased estimator of trace(P) [5], which is k. In fact, with $\tilde{z} = Q^T z$, it is known that $\xi_N^{(2)} = \|\tilde{z}_{1:k}\|_2^2$ follows the χ_k^2 distribution (the χ^2 distribution with k degrees of freedom). The expectation and variance results then follow. For the probability, here we simply use $\xi_N^{(2)} \geq \tilde{z}_1^2$ so as to obtain a bound independent of k. (The tail probability of the χ_k^2 distribution will be used in the next theorem to get a tighter bound for larger k.) Since $\tilde{z}_1^2$ follows the χ_1^2 distribution, standard results on the χ_1^2 distribution and the error function (erf) yield $\Pr(\xi_N^{(2)} \leq \varepsilon) \leq \Pr(\tilde{z}_1^2 \leq \varepsilon) = \mathrm{erf}(\sqrt{\frac{\varepsilon}{2}})$. By using an inequality for the error function in [41], the final probability bound is then obtained. □

In Theorem 4, the probability bound does not depend on k. We may get a bound that decreases for increasing k based on $\|Pz\|_2$ as an estimator.

Theorem 5 *Suppose there are $k \geq 1$ eigenvalues in the interval enclosed by $\mathscr{C}$. Let $z \sim \mathcal{N}(0, I_n)$ and $\xi_N^{(1)} = \|Pz\|_2$. Then for $0 < \varepsilon < 1$,*

$$\sqrt{k-1} < \mathrm{E}(\xi_N^{(1)}) \leq \sqrt{k}, \quad \mathrm{Var}(\xi_N^{(1)}) < 1, \quad \Pr(\xi_N^{(1)} \leq \varepsilon) \leq \exp\left(-\frac{k}{4}\left(1 - \frac{\varepsilon^2}{k}\right)^2\right).$$

Proof Again, $\xi_N^{(2)} = \|Pz\|_2^2$ follows the χ_k^2 distribution and has probability density function $\frac{t^{k/2-1}e^{-t/2}}{2^{k/2}\Gamma(k/2)}$. Then the standard expectation computation yields

$$\mathrm{E}(\xi_N^{(1)}) = \int_0^\infty t^{1/2} \frac{t^{k/2-1}e^{-t/2}}{2^{k/2}\Gamma(k/2)} dt = \sqrt{2}\frac{\Gamma((k+1)/2)}{\Gamma(k/2)}.$$

We can then obtain the following bounds similarly to (7):

$$\sqrt{\frac{k-1}{2}} < \frac{\Gamma((k+1)/2)}{\Gamma(k/2)} \leq \sqrt{\frac{k}{2}}.$$

The result on $\mathrm{E}(\xi_N^{(1)})$ then follows. Also,

$$\mathrm{Var}(\xi_N^{(1)}) = \mathrm{E}(\xi_N^{(2)}) - (\mathrm{E}(\xi_N^{(1)}))^2 = k - (\mathrm{E}(\xi_N^{(1)}))^2 < k - (k-1) = 1.$$

The probability bound is due to a tail probability bound of the χ_k^2 distribution in [22, Lemma 1]. That is, for any $\alpha > 0$,

$$\Pr(\xi_N^{(2)} \leq k - 2\sqrt{k\alpha}) \leq \exp(-\alpha).$$

Setting $k - 2\sqrt{k\alpha} = \varepsilon^2$ yields $\alpha = \frac{k}{4}\left(1 - \frac{\varepsilon^2}{k}\right)^2$. Then $\Pr(\xi_N^{(1)} \leq \varepsilon) = \Pr(\xi_N^{(2)} \leq \varepsilon^2) \leq \exp(-\alpha)$. □

In the next subsection, we will give a comparison of the quality of the estimators and then use them in the design of reliable eigenvalue indicators.

Remark 1 As in many other randomized methods, the reliability of the estimators can be improved via the use of multiple random vectors. For example, if z_i, $i = 1, \ldots, \tilde{m}$ are random vectors independently and uniformly selected from S_{n-1}, then we may replace $\xi_U^{(1)}$ by the estimator $\tilde{\xi}_U^{(1)} = \frac{1}{\tilde{m}} \sum_{i=1}^{\tilde{m}} \|Pz_i\|_2$ to still get $\mathrm{E}(\tilde{\xi}_U^{(1)}) \geq \sqrt{k}\omega_n$ like in Theorem 2. Moreover, the reliability result in Theorem 2 improves:

$$\Pr(\tilde{\xi}_U^{(1)} \leq \varepsilon) \leq \Pr(\frac{1}{\tilde{m}} \sum_{i=1}^{\tilde{m}} |q_1^T z_i| \leq \varepsilon) = \Pr(\frac{1}{\tilde{m}\omega_n} \sum_{i=1}^{\tilde{m}} |q_1^T z_i| \leq \frac{\varepsilon}{\omega_n}) \leq \frac{1}{\tilde{m}!}\left(\frac{2\tilde{m}\varepsilon}{\pi\omega_n}\right)^{\tilde{m}},$$

where the last inequality is from [21, Theorem 2.4]. For example, with $\tilde{m} = 2$, the probability bound above is $2\left(\frac{2\varepsilon}{\pi\omega_n}\right)^2$ in contrast with the bound $\frac{2\varepsilon}{\pi\omega_n}$ in Theorem 2.

Similarly, if z_i, $i = 1, \ldots, \tilde{m}$ are independent standard Gaussian random vectors, then we may replace $\xi_N^{(1)}$ in Theorem 5 by the estimator $\tilde{\xi}_N^{(1)} = \frac{1}{\tilde{m}} \sum_{i=1}^{\tilde{m}} \|Pz_i\|_2$ to still have $\sqrt{k-1} < \mathrm{E}(\tilde{\xi}_N^{(1)}) \leq \sqrt{k}$. Now, the reliability result also improves. In fact, $\tilde{\xi}_N^{(1)} \geq \frac{1}{\tilde{m}}\sqrt{\sum_{i=1}^{\tilde{m}} \|Pz_i\|_2^2}$ so that we can apply the tail probability bound of the $\chi_{\tilde{m}k}^2$ distribution to get

$$\Pr(\tilde{m}^2(\tilde{\xi}_N^{(1)})^2 \leq \tilde{m}k - 2\sqrt{\tilde{m}k\alpha}) \leq \exp(-\alpha).$$

Setting $\frac{\tilde{m}k-2\sqrt{\tilde{m}k\alpha}}{\tilde{m}^2}=\varepsilon^2$ yields $\alpha=\frac{\tilde{m}k}{4}\left(1-\frac{\tilde{m}\varepsilon^2}{k}\right)^2$. Then

$$\Pr(\tilde{\xi}_N^{(1)}\le\varepsilon)=\exp\left(-\frac{\tilde{m}k}{4}\left(1-\frac{\tilde{m}\varepsilon^2}{k}\right)^2\right).$$

This shows how the probability bound in Theorem 5 improves as $\tilde{m}$ increases.

However, it is worth pointing out that, using multiple z_i requires to significantly increase the cost for evaluating the estimators when Krylov subspace methods like in Section 3 are used. This is because each z_i requires to form a new Krylov subspace like in (17) below. In this work, one random vector is used since it is very efficient and already gives reasonably nice reliability.

2.2 Rejection indicators

For the purpose of designing a robust rejection indicator, we would like to compare the estimators ξ in the previous subsection. Table 1 summarizes the behaviors of the estimators. We can make the following observations, where we assume n is not too small.

- For the estimator $\xi_U^{(1)}$, we can compare the results in Theorems 1 and 2. Since $\omega_n=\sqrt{\frac{2}{\pi(n-1/2)}}+O(n^{-3/2})$ [21], for large n, the lower bound of $\mathrm{E}(\xi_U^{(1)})$ in Theorem 2 is about $\sqrt{\frac{2k}{\pi n}}$, the upper bound of $\mathrm{Var}(\xi_U^{(1)})$ is about $(1-\frac{2}{\pi})\frac{k}{n}$, and the upper bound of $\Pr(\xi_U^{(1)}\le\varepsilon)$ is about $\varepsilon\sqrt{\frac{2n-1}{\pi}}$. For $k>2$, $\mathrm{E}(\xi_U^{(1)})$ in Theorem 2 has a slightly smaller lower bound than that in Theorem 1. For $k=1$ or 2, $\mathrm{Var}(\xi_U^{(1)})$ in Theorem 2 has a smaller upper bound. For larger n, the result $\mathrm{Var}(\xi_U^{(1)})<\frac{1}{n}$ in Theorem 1 is more satisfactory and is further independent of k. The failure probability bound in Theorem 2 is about the same as that in Theorem 1.
- The expectations for all the estimators increase with k. The expectations for the estimators $\xi_N^{(1)}$ and $\xi_N^{(2)}$ are further independent of n.
- The variances for $\xi_U^{(1)}$ and $\xi_U^{(2)}$ are relatively small.
- About the failure probabilities $\Pr(\xi\le\varepsilon)$, the following can be concluded.
  - The failure probabilities for all the estimators get smaller as ε decreases. The probability bounds for $\xi_U^{(1)}$, $\xi_U^{(2)}$, and $\xi_N^{(2)}$ all go to 0 as $\varepsilon\to 0$.
  - The probability bounds for $\xi_U^{(1)}$ and $\xi_N^{(2)}$ are independent of k. The probability bounds for $\xi_U^{(2)}$ and $\xi_N^{(1)}$ decrease when k gets larger. As k increases, the probability bound for $\xi_U^{(2)}$ quickly gets very small.
  - The probability bounds for $\xi_N^{(1)}$ and $\xi_N^{(2)}$ are also independent of n.

Table 1 Summary of the analysis in Theorems 1–5.

z	Estimator ξ	$\mathrm{E}(\xi)$	$\mathrm{Var}(\xi)$	$\Pr(\xi\le\varepsilon)$
$z\in\mathscr{U}(S_{n-1})$	$\xi_U^{(1)}=\|Pz\|_2$	$(\sqrt{\frac{k-1}{n}},\sqrt{\frac{k}{n}}]$	$<\frac{1}{n}$	$\le\varepsilon\sqrt{\frac{2n}{\pi}}$
	$\xi_U^{(1)}=\|Pz\|_2$	$\ge\sqrt{k}\omega_n$	$\le\frac{k}{n}-k\omega_n^2$	$\le\frac{2\varepsilon}{\pi\omega_n}$
	$\xi_U^{(2)}=\|Pz\|_2^2$	$\frac{k}{n}$	$\frac{2k(n-k)}{n^2(n+2)}$	$<\sqrt{\frac{2}{k\pi}}\left(\varepsilon(n+1-k)\right)^{k/2}$
$z\sim\mathscr{N}(0,I_n)$	$\xi_N^{(1)}=\|Pz\|_2$	$(\sqrt{k-1},\sqrt{k}]$	<1	$\le\exp\left(-\frac{k}{4}\left(1-\frac{\varepsilon^2}{k}\right)^2\right)$
	$\xi_N^{(2)}=\|Pz\|_2^2$	k	$2k$	$\le\sqrt{1-\exp(-\frac{2}{\pi}\varepsilon)}$

For some n and ε values, we plot the bounds for $\Pr(\xi\le\varepsilon)$ in Figure 1. It can be seen that at least one of the estimators gives very small failure probability. Moreover, as k increases, some failure probability bounds quickly approach 0.

According to these discussions, we can conclude the following when $k\ge 1$ or there is at least one eigenvalue inside the interval.

1. Some of the estimators have expectations at least 1 and the expectations grow with k.

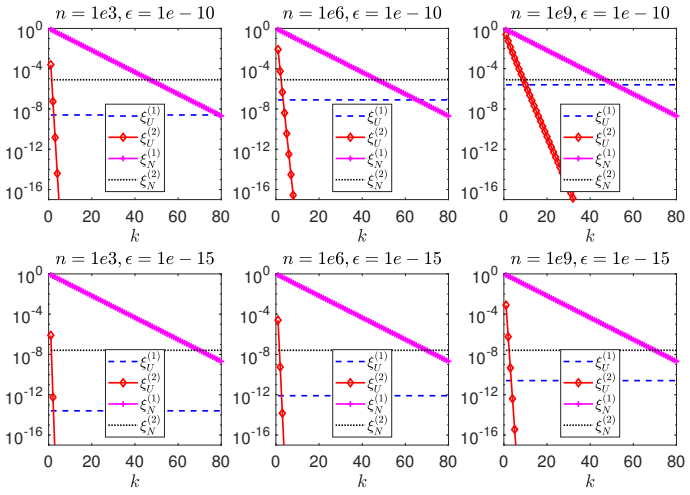

Fig. 1 Upper bounds for the failure probabilities $\Pr(\xi \le \varepsilon)$ with different estimators ξ, where the plot for $\xi_U^{(1)}$ is based on the bound in Theorem 2 since the one in Theorem 1 is similar.

2. Moreover, the probabilities for the estimators to return estimates smaller than a tiny threshold ε are very low. Even if k is as small as 1, at least one estimator has a reasonably small failure probability.
3. In addition, when k is large, some failure probabilities are extremely small.

Based on these, we can design a rejection indicator in either of the following ways.

– Set the failure probability bound to be a small number and then use our probability analysis to decide the corresponding ε as a threshold for the estimators.
– We may also directly set a small ε (such as 10^{-15}) as the threshold for the estimators.

Here, we follow the second way since the discussions above indicate that, if one of the estimators $(\xi_N^{(1)}, \xi_N^{(2)}, \xi_U^{(1)}, \xi_U^{(2)})$ returns a value smaller than ε, then the probability of having an eigenvalue inside the interval is extremely low. Also see Figure 1. That is, we claim there is no eigenvalue inside the interval if

$$\xi_R \equiv \min\{\xi_N^{(1)}, \xi_N^{(2)}, \xi_U^{(1)}, \xi_U^{(2)}\} < \varepsilon. \tag{8}$$

For convenience, we say (8) is a *safe rejection indicator*, which is a key indicator in our method. Although this design looks simple, its effectiveness is built upon the rigorous statistical justifications above.

Remark 2 In our analysis, we have studied estimators with both $z \sim \mathscr{U}(S_{n-1})$ and $z \sim \mathscr{N}(0, I_n)$ in order to compare the failure probabilities. When the estimators are used for the actual design of the indicator in (8), the minimum is much more likely achieved by $\xi_U^{(1)}$ or $\xi_U^{(2)}$ because of the different magnitudes of the estimators. This may be seen as follows. Suppose $\xi_N^{(1)} = \|Pz\|_2$ is computed with $z \sim \mathscr{N}(0, I_n)$. Then

$$\xi_N^{(2)} = (\xi_N^{(1)})^2, \quad \xi_U^{(2)} = \frac{1}{\|z\|_2^2}\xi_N^{(2)}, \quad \xi_U^{(1)} = \sqrt{\xi_U^{(2)}}. \tag{9}$$

Note $\|z\|_2^2 = \mathrm{E}(n)$. $\xi_U^{(1)}$ or $\xi_U^{(2)}$ is likely smaller. Similarly, in the acceptance indicator (10) below, the maximum is more likely achieved by $\xi_N^{(1)}$ or $\xi_N^{(2)}$. On the other hand, (9) also indicates that, once one of the estimators is available, the others are available with almost no extra cost. Thus, in both (8) above and (10) below, we consistently include all the four estimators without excluding those rare cases (like when ξ_R is achieved by $\xi_N^{(1)}$ or $\xi_N^{(2)}$ because of particular small $\|z\|_2$).

In our proposed eigenvalue detection strategy, if the interval is not rejected by the safe rejection indicator, it is not automatically accepted. Instead, we may further apply some acceptance indicators in the next subsection. If all those acceptance indicators fail to indicate that there are eigenvalues inside the interval, then we still claim there is no eigenvalue inside. This also leads to a rejection indicator, called a *passive rejection indicator*.

As mentioned above, our failure probability bounds can be conveniently controlled and made almost 0. Theoretically, a single z may happen to not include the eigenvector component for an eigenvalue. However, the probability is 0 because of the randomness of z.

2.3 Acceptance indicators

We may then accept an interval if it is not rejected by our safe rejection indicator. On the other hand, we may further confirm the eigenvalue existence by applying some acceptance indicators (as auxiliary indicators). This sometimes saves a small amount of costs. We point out that, since this is an additional layer of safeguard, we use a set of criteria where the threshold is conservative and is not as rigorously derived as in the safe rejection indicator. (Anyway, it is sometimes less problematic to accept an interval without eigenvalues than to incorrectly reject an interval with eigenvalues. Often, an incorrectly accepted interval will eventually get discarded in further interval refinements due to a self-correction effect mentioned in Section 3.2 below.)

The acceptance indicators we use are as follows.

- When there are $k \geq 1$ eigenvalues inside the interval, the estimators $\xi_N^{(1)}$, $\xi_N^{(2)}$, $\xi_U^{(1)}$, $\xi_U^{(2)}$ have expectations as given in Section 2.1. Since the maximum of the expectations is k, we claim there are eigenvalues within the interval if the maximum of the numerical estimates is larger than or equal to a threshold $\eta \in (0,1)$:

$$\max\{\xi_N^{(1)}, \xi_N^{(2)}, \xi_U^{(1)}, \xi_U^{(2)}\} \geq \eta. \tag{10}$$

- We also follow the strategy in [18] to define an acceptance indicator. That is, suppose the numerical application of P in (1) to z is performed via a quadrature rule with both m points and $m/2$ points, with the resulting approximations y_m and $y_{m/2}$ to $\|Pz\|_2$, respectively. (Equation (13) below shows a specific form.) Then, $y_m/y_{m/2}$ is expected to be close to 1 if $k \geq 1$ and close to 0 otherwise. For some quadrature rules, this is because of the fast error decay (see, e.g. [37]). Thus, we let m_0 be the starting number of quadrature points and $m = 2^l m_0$ and compute the length-$(l+1)$ vector

$$\rho = \begin{pmatrix} y_{m_0} & y_{2m_0} & \cdots & y_{m/2} & y_m \end{pmatrix}^T. \tag{11}$$

  Now the interval is accepted if

$$\max_{1<i\leq l} \frac{\rho_{i+1}}{\rho_i} \geq \eta \quad \text{or} \quad \frac{1}{l}\sum_{i=1}^{l} \frac{\rho_{i+1}}{\rho_i} \geq \eta. \tag{12}$$

These two acceptance indicators can be viewed as extended versions of those in [17–19]. Following the choice of a threshold in [18] based on extensive numerical tests, we may set η in both (10) and (12) to be, say, 0.2. In our tests in Section 4, if a subinterval is not rejected by the safe rejection indicator at the first place, it is usually also accepted next by one of the acceptance indicators with $\eta = 0.2$.

3 A prototype framework for symmetric eigenvalue detection and eigenvector solution with the indicators

We now present one prototype framework to illustrate how our indicator method may be applied numerically for eigenvalue detection and how it may potentially be useful for designing innovative randomized eigenvalue and eigenvector solvers.

Remark 3 We would like to emphasize the following.

1. The resulting eigenvalue detection strategy works for general symmetric matrices. However, it is *not* our aim here to optimize its design or to produce an already highly competitive general-purpose eigensolver. The design of practical efficient eigensolvers takes extensive research efforts and careful implementations which are far beyond this work. Thus, some components of the eigensolver may not necessarily be refined, including the quadrature approximation of $\|Pz\|_2$, the choice of a preconditioner in the indicator evaluation, and the tuning of some parameters.
2. The purpose of this work is to illustrate that randomization may be made reliable for designing accurate eigensolvers. The resulting algorithm serves as a proof-of-concept model to show a new route to expand the applicability of randomization to eigenvalue methods which are usually overlooked in randomized linear algebra.
3. Like other eigenvalue methods for general symmetric matrices, the performance of our presented methods is problem dependent.

3.1 Indicator evaluation

The main computation in the detection of the existence of eigenvalues within an interval (a,b) is the evaluation of the indicators, which comes to the approximate numerical evaluation of $\|Pz\|_2$ with an appropriate quadrature rule. Note that it is *not* necessary to form Pz itself. There are lots of studies of the effectiveness of quadrature rules for the purpose of eigenvalue filtering in previous contour-integral eigensolvers [15,39,47]. For example, we may follow [18, 47] and use the trapezoidal rule for convenience. (Here, since we only need the indicators to make a $0/1$ judgement of eigenvalue existence, it would be interesting to study the impact of quadrature rules in future work.) Set $\mathscr{C}$ to be a circle with center c of (a,b) and radius $r=\frac{b-a}{2}$. Let $s_j = c + re^{\frac{2j\pi\mathbf{i}}{m}}, j = 0,1,\ldots,m-1$ be the quadrature nodes. Then the trapezoidal approximation looks like

$$\|Pz\|_2 = \|\frac{1}{2\pi\mathbf{i}}\int_{\mathscr{C}}(sI-A)^{-1}zds\|_2 \approx \frac{1}{m}\|\sum_{j=0}^{m-1}(A-s_jI)^{-1}z\|_2. \tag{13}$$

The estimation of $\|Pz\|_2$ eventually arrives at the following shifted linear systems with a fixed right-hand side:

$$(A-s_jI)x_j = z. \tag{14}$$

There are various iterative solvers that can reuse Krylov subspaces for multiple shifts. See, e.g., [2,11,35].

However, we can quickly evaluate $\|Pz\|_2$ *without solving for the explicit solution* x_j. The idea is to combine preconditioning with the Lanczos method, following a Cayley transformation strategy in [18] (originally for nonsymmetric matrices). We outline the main steps without going into detailed derivations. Associated with the center c of the interval, let

$$C = (A-cI)^{-1}, \tag{15}$$

which is precomputed via a pivoted LDL factorization and will serve as a preconditioner for the solution of (14). (We may also use approximate LDL factorizations like those in [44,45].) The preconditioned linear system looks like

$$C(A-s_jI)x_j = (I+(c-s_j)C)x_j = f \quad \text{with} \quad f = Cz. \tag{16}$$

Let d be a small integer and use Lanczos iterations to generate a Krylov subspace

$$\mathscr{K}_d(C,f) = \text{span}\{f, Cf, \ldots, C^{d-1}f\}. \tag{17}$$

It is clear that $\mathscr{K}_d(I+(c-s_j)C,f) = \mathscr{K}_d(C,f)$.

Lanczos iterations produce a sequence of orthonormal vectors $v_1,\ldots,v_d,v_{d+1}$ and a $d\times d$ tridiagonal matrix T_k such that

$$CV_d = V_dT_d + hv_{d+1}e_d^T,$$

where $V_d = (\,v_1\ \cdots\ v_d\,)$, h is a scalar, and e_d is the d-th natural basis unit vector. Compute an eigenvalue decomposition for the *small* tridiagonal matrix T_d:

$$T_d = Q_dD_dQ_d^T. \tag{18}$$

Then an iterative solution to (16) looks like (see, e.g., [30] for the detailed derivation)

$$x_j = \|f\|_2V_dQ_du_j \quad \text{with} \tag{19}$$

$$u_j = (I+(c-s_j)D_d)^{-1}(Q_d^Te_1). \tag{20}$$

Note u_j instead of x_j is explicitly formed since we just need to evaluate the norm in (13).

The residual can be conveniently evaluated based on results on the Lanczos method [30] and also [18]:

$$\mathbf{r} = |((c-s_j)h\|f\|_2)p_d^Tu_j|, \tag{21}$$

where $p_d^T = e_d^TQ_d$ is the d-th row of Q_d. (We may also use the relative residual $|((c-s_j)h)p_d^Tu_j|$.) Thus, we can quickly compute the residual through the length-d dot product in (21). This shows it is convenient to assess the quality of the preconditioner as needed in the next subsection.

With u_j in (20), $\|Pz\|_2$ in (13) can be approximated as

$$\|Pz\|_2 \approx \frac{1}{m}\|\sum_{j=0}^{m-1}x_j\|_2 = \frac{1}{m}\|f\|_2\|\sum_{j=0}^{m-1}V_dQ_du_j\|_2 = \frac{\|f\|_2}{m}\|\sum_{j=0}^{m-1}u_j\|_2, \tag{22}$$

From this, it is clear that we only need to store two length-d vectors (the diagonal of D_d and the first row of Q_d) as needed in (20) and there is no need to store x_j or the Krylov subspace basis vectors (unless eigenvectors are needed). This feature is also explored in [19].

Another thing worth mentioning is that the acceptance indicators in Section 2.3 need to compute approximations with different numbers of quadrature points. (22) shows how y_m in (11) is obtained. When the number of quadrature points doubles from $m/2$ to m, the evaluation of y_m can reuse computations from the evaluation of $y_{m/2}$.

3.2 Eigenvalue detection and solution

To find all the eigenvalues within an interval (a,b), we can repeatedly bisect the interval and apply the indicator evaluation as in the previous subsection (with the preconditioner C reused) to determine if there are eigenvalues inside the subintervals. This is done until there is no eigenvalue inside a subinterval or the subinterval size is smaller than a given tolerance τ:

$$|b-a| \leq \tau. \tag{23}$$

For the latter case, return $c = \frac{a+b}{2}$ as an eigenvalue (that satisfies the prespecified accuracy τ). This is somewhat similar to the inertia-based bisection eigensolver [28]. Note that since the eigenvalue is found only based on the detection of eigenvalue existence, if there is a repeated eigenvalue in the interval, the eigensolver typically returns the eigenvalue as a single one and does not see the multiplicity. For strategies to detect eigenvalue multiplicity based on the extraction of eigenspace information, see [46] for an extension of the current work. One way is to find eigenvectors via multiple z vectors. See Example 5 below.

When (a,b) is repeatedly bisected, like in [18] (for non-symmetric matrices), the preconditioner C may be reused for multiple descendant subintervals in the hierarchical partitioning, and even for some nearby subintervals if scalability is not the concern. The quality of C may be quickly assessed through (21). When a descendant or nearby subinterval is not too far away from c, C is expected to be effective for the shifted linear systems associated with the subinterval. Otherwise, a new preconditioner and a new Krylov subspace might be needed. This process thus tries to reuse computations as much as possible across indicator evaluations, similarly to the bisection methods in [13,44] that reuse computations for multiple inertia evaluations.

Note that eigenvalue detection may be performed simultaneously for different subintervals at the same level of the partitioning, similarly to the bisection method and other contour-integral eigensolvers.

Unlike in the standard Lanczos eigensolver (see, e.g., [31]), here d in (17) is usually set to be very small and just enough to give a reasonable evaluation of the indicators. The convergence of the eigenvalues is controlled by the bisection process instead of Lanczos iterations. Also, one Krylov subspace here may potentially be used to find multiple eigenvalues in different intervals.

The cost of the overall bisection process can be counted as follows. Let N_{Kr} be the total number of Krylov subspaces generated in the process, N_{bis} be the total number of visited subintervals, θ_{prec} be the number of flops to compute the preconditioner in (15), and θ_{sol} be the number of flops to apply C in (15) to a vector via the LDL factors. Then the complexity to generate all the Krylov subspaces is $\phi_0 = N_{\text{Kr}}(\theta_{\text{prec}} + d\theta_{\text{sol}} + O(dn+d^3))$, where $O(dn+d^3)$ is mainly for appropriate vector operations in the Lanczos iterations and for the eigenvalue decomposition of each T_d. When the preconditioner quality is high, ϕ_0 may be viewed as a precomputation cost.

The cost to evaluate $\|Pz\|_2$ is just $O(md)$ through the evaluation of $\|\sum_{j=0}^{m-1} u_j\|_2$. Then the complexity to evaluate the indicators in all the bisection steps for finding the eigenvalues in the interval (a,b) is

$$\phi = N_{\text{bis}} O(md) = O(kmd \log \frac{b-a}{\tau}). \tag{24}$$

That is, it only costs $O(md \log \frac{b-a}{\tau})$ per eigenvalue. With given interval and τ and with m and d typically small, the cost per eigenvalue is quite small. The extensive numerical experiments in Section 4 confirm that small m and d are sufficient to perform reliable eigenvalue detection.

In the evaluation of the indicators, both the quadrature approximation and the Krylov subspace method involve approximation errors. The precise quantification of how these errors impact the indicator quality will be left for future investigations. Our tests below indicate the eigenvalue detection is relatively robust with respect to these errors and some parameters. In fact, when $k \geq 1$, it is unlikely for the approximation errors to happen to make $\|Pz\|_2$ smaller than our prespecified threshold ε (such as 10^{-15}). When $k = 0$, the indicators may initially accept a large interval without eigenvalues since the quadrature approximation is less accurate. With the interval further refined, the quadrature points get closer so that the quadrature approximation likely gets more accurate. Then the estimators will eventually return small estimates so as to reject the subintervals. This is a self-correction effect which has also been observed previously in the preliminary indicator method in [17].

For convenience, Algorithm 1 shows the eigenvalue solution framework with the robust indicator method.

Remark 4 If an eigenvalue happens to be on the boundary of $[a,b]$ that is circumscribed by the circle $\mathscr{C}$, the (numerical) indicators would likely suggest the existence of eigenvalues in the interval (so that an approximate eigenvalue within distance τ of that boundary eigenvalue would eventually be returned in later refinements). This is because of the behavior of the quadrature rule in filtering eigenvalues [15,39,47]. Roughly speaking, the quadrature rule (as a filter function) returns a numerical estimate that is not very small at the boundary. The filter function quickly decays to 0 only when it is evaluated at points away from the interval. Example 5 below includes a test for such a situation.

Algorithm 1 Robust indicator eigensolver

procedure eigindc(A, a, b, τ) ▷ *Indicator eigensolver framework similar to that in [18] for finding the eigenvalues in* (a,b)
  $c \leftarrow \frac{a+b}{2}$, $r \leftarrow \frac{b-a}{2}$
  if there are previously constructed Krylov subspaces **then**
    Use (21) for quick accuracy check to identify a previous Krylov subspace (17)
  end if
  if there is no previously constructed Krylov subspace or if none of the subspaces satisfy the accuracy requirement **then**
    Construct a new Krylov subspace (17) with C in (15) and f in (16) ▷ $f = Cz$ *with* z *a standard Gaussian random vector*
  end if
  Find D_d, Q_d in (18) for the identified Krylov subspace
  $\mathscr{I} \leftarrow$ indc(A, c, r, D_d, Q_d, f) ▷ *Indicator evaluation*
  if $\mathscr{I} = 1$ **then**
    if $b - a \le \tau$ **then**
      Return c as a (numerical) eigenvalue
    else
      Run eigindc(A, a, c, τ) and eigindc(A, c, b, τ) ▷ *Bisection*
    end if
  end if
end procedure

---

procedure indc(A, c, r, D_d, Q_d, f) ▷ *Robust eigenvalue detection with the rejection and acceptance indicators*
  for $i = 0, 1, \ldots, l$ **do** ▷ l*: a specified power such as* 4
    $m_i \leftarrow 2^i m_0$ ▷ m_0*: initial number of quadrature points such as* 2
    Evaluate all u_j in (20) with D_d, Q_d, and quadrature points $s_j = c + re^{\frac{2j\pi\mathbf{i}}{m_i}}$
    $\rho_{i+1} \leftarrow \frac{\|f\|_2}{m_i} \|\sum_{j=0}^{m_i-1} u_j\|_2$ ▷ *Entries of* ρ *in (11):* $\rho_{i+1} = y_{m_i}$*, which may also be updated from* ρ_i *to save cost*
  end for
  $\xi_N^{(1)} \leftarrow \rho_{l+1}$; obtain $\xi_N^{(2)}, \xi_U^{(1)}, \xi_U^{(2)}$ as in (9)
  if $\min\{\xi_N^{(1)}, \xi_N^{(2)}, \xi_U^{(1)}, \xi_U^{(2)}\} < \varepsilon$ **then** ▷ *Safe rejection indicator with threshold* ε *such as* 10^{-15}
    $\mathscr{I} \leftarrow 0$; return $\mathscr{I}$
  end if
  if $\max\{\xi_N^{(1)}, \xi_N^{(2)}, \xi_U^{(1)}, \xi_U^{(2)}\} \ge \eta$, $\max_{1<i\le l} \frac{\rho_{i+1}}{\rho_i} \ge \eta$, or $\frac{1}{l}\sum_{i=1}^{l} \frac{\rho_{i+1}}{\rho_i} \ge \eta$ **then** ▷ *Acceptance indicators with threshold* η *such as* $\frac{1}{5}$
    $\mathscr{I} \leftarrow 1$; return $\mathscr{I}$
  else ▷ *Passive rejection indicator*
    $\mathscr{I} \leftarrow 0$; return $\mathscr{I}$
  end if
end procedure

3.3 Eigenvector computation and extension to generalized eigenvalue problems

Now, suppose a numerical eigenvalue $\tilde{\lambda}_j$ has been identified. The previous indicator methods in [17–19] are not able to find an eigenvector corresponding to $\tilde{\lambda}_j$. Here, we can actually reuse the computations in the indicator evaluation to also find an approximate eigenvector $\tilde{q}_j$. That is, based on the preconditioned Lanczos method in the previous subsection, $\tilde{q}_j$ can be conveniently obtained with little extra cost.

The idea is to simply apply one step of inverse iteration and evaluate the vector $\hat{q}_j = (A - \tilde{\lambda}_j I)^{-1} z$ and then normalize it to get $\tilde{q}_j$. (Classical studies of the inverse iteration ensures the reliability of $\tilde{q}_j$.) That is, we solve the following system for $\hat{q}_j$:

$$(A - \tilde{\lambda}_j I)\hat{q}_j = z.$$

Obviously, this has the same form as (14), except with the shift s_j replaced by $\tilde{\lambda}_j$. Thus, we can directly replace s_j in (19) by $\tilde{\lambda}_j$ and then $\hat{q}_j$ is just x_j:

$$\hat{q}_j = \|f\|_2 V_d(Q_d \tilde{u}_j),$$

where $\tilde{u}_j$ comes from (20) with s_j replaced by $\tilde{\lambda}_j$. Now, set the approximate eigenvector $\tilde{q}_j = \frac{\hat{q}_j}{\|\hat{q}_j\|_2}$.

The computation cost for the above procedure is just $O(dn + d^2)$, which is $O(n)$ with d fixed. Thus, this provides a very convenient and efficient way to extract $\tilde{q}_j$. Of course, here the Lanczos basis vectors in V_d in (19) need to be stored. Q_d also needs to be stored, but it is small.

The eigenvalue detection strategy can be immediately extended to generalized eigenvalue problems of the form $Aq = \lambda Bq$ with symmetric A and symmetric positive definite B. The main changes are as follows. Replace I in (13)–(16) by B. Then the preconditioned system (16) becomes

$$(I + (c - s_j)\hat{C}B)x = \hat{f} \quad \text{with} \quad \hat{C} = (A - cB)^{-1}, \quad \hat{f} = \hat{C}z$$

Thus, the Krylov subspace in (17) needs to be replaced by $\mathscr{K}_d(\hat{C}B, \hat{f})$, which is already used in [18].

Here, $\hat{C}B$ is generally nonsymmetric, so Arnoldi iterations are used to generate a set of orthonormal basis vectors $v_1, v_2, \ldots, v_{d+1}$ and a $d \times d$ upper Hessenberg matrix T_k. Then the remaining steps for the shifted linear system solution can proceed similarly to those in Section 3.1. Note that we may revise the scheme so that symmetry is preserved and Lanczos iterations can still be used. That is, if B has a Cholesky factorization $R^T R$, then we may replace A in Section 3.1 by $R^{-T}AR^{-1}$. Now since

$$(R^{-T}AR^{-1} - cI)^{-1} = R\hat{C}R^T,$$

we can then replace $\mathscr{K}_d(C, f)$ in (17) by $\mathscr{K}_d(R\hat{C}R^T, f)$, where symmetry is preserved in $R\hat{C}R^T$. Here, since d is usually small, it may be preferable to simply use Arnoldi iterations to form $\mathscr{K}_d(\hat{C}B, \hat{f})$ so as to avoid the factorization of B. This is what we follow in the numerical experiments below.

4 Numerical experiments

We now test our indicator method for eigenvalue detection and also compare with some other methods, especially the indicator method in [18, 19]. We point out that the tests intend to show the reliability of the eigenvalue detection. They indicate the potential of designing new indicator-based eigensolvers in the future. Our focus is *not* yet to implement a highly efficient or practical eigensolver or to compare with existing state-of-the-art eigensolvers.

To facilitate the display of the results, we collect the frequently used notation as follows.

- NEW: the new symmetric eigenvalue detection strategy based on the indicators in this work.
- SIM: the symmetric eigenvalue detection strategy based on the indicator used in the original indicator method (called spectral indicator method) in [18, 19]. (Here specifically for symmetric matrices, we use our implementation but with the indicator given in [18, 19] which is just (3).)
- ε: the rejection tolerance in (8) in NEW.
- δ: the rejection tolerance in (3) in SIM.
- τ: the accuracy of the eigenvalue solution as controlled by the stopping criterion (23).
- d: the maximum dimension of each Krylov subspace as in (17).
- N_{Kr}: the number of Krylov subspaces (17) needed.
- k: the number of eigenvalues within an interval (either in the exact sense or as reported by an eigensolver).
- λ_i: true eigenvalues as obtained by either the Matlab function eig (or eigs if n is large and eigs works).
- $\tilde{\lambda}_i$: numerical approximation to λ_i.
- $E = \max_i |\lambda_i - \tilde{\lambda}_i|$: eigenvalue error measurement. (Absolute errors are measured since the stopping criterion is based on interval sizes.)
- $\gamma = \max_i \frac{\|A\tilde{q}_i - \tilde{\lambda}_i B\tilde{q}_i\|_2}{\|A\|_2\|\tilde{q}_i\|_2 + |\tilde{\lambda}_i|\|B\|_2\|\tilde{q}_i\|_2}$: residual measurement for the eigenvalue problem $Aq = \lambda Bq$. Since we normalize the eigenvectors, essentially $\|\tilde{q}_i\|_2 = 1$. If it is a standard eigenvalue problem, then $B = I$.

In NEW, we can use ε to conveniently control the failure probability of estimators used by the rejection indicator. For reliability, we set $\varepsilon = 10^{-15}$ in most of the tests, unless otherwise specified. For the acceptance estimators in NEW, a threshold $\eta = 0.2$ is used in (10) and (12). For reliability, we set the maximum number of quadrature points $m = 32$ in (11), where $m_0 = 2$. In the preconditioned Lanczos solution of the shifted linear systems, we use 10^{-6} as the residual tolerance for checking whether a new preconditioner is needed or not. With the same k and τ, the dominant costs of NEW and SIM are controlled by N_{Kr}. In most of the tests below, NEW and SIM have similar N_{Kr} counts.

In each example below, we try to detect some interior or extreme eigenvalues with a same random vector z. Tests with randomly selected search intervals and different z are also included. The timing results are obtained in Matlab on a node of the Purdue Brown Cluster using 2 cores and 36GB of memory.

Example 1 In this first example, we consider the symmetric matrix A from the example `bodyy6` in the SuiteSparse sparse matrix collection [34]. A has size $n = 19,366$ and $134,208$ nonzero entries. We treat the results from eig in Matlab as the true eigenvalues λ_i.

We first look at randomly selected intervals to demonstrate the reliability of the indicators in deciding eigenvalue existence. For an indicator applied to M intervals of length s and with center in $(-\|A\|_1, \|A\|_1)$, we look at the ratios $\mathscr{R}_0$, $\mathscr{R}_+$, and $\mathscr{R}_-$ of *correct, over, and under detections*, respectively:

- $\mathscr{R}_0$: ratio of cases where the indicator correctly tells if there are eigenvalues inside or not,
- $\mathscr{R}_+$: ratio of cases where the indicator accepts intervals without eigenvalues inside, and
- $\mathscr{R}_-$: ratio of cases where the indicator rejects intervals with eigenvalues inside.

Here, $\|A\|_1 \approx 9.8 \times 10^4$ and we test a sequence of lengths $s = 10^{-10}, 10^{-9}, \ldots, 10^4$ and randomly choose $M = 1000$ intervals for each length s. Set $d = 50$. The ratios from the SIM and NEW indicators are reported in Figure 2. $\delta = 0.4$ is used in SIM and similar results are also obtained with other δ values. For SIM, the $\mathscr{R}_0$ ratios are low and the $\mathscr{R}_+$ ratios are high for most s sizes, indicating a substantial chance of over-detection. $\mathscr{R}_-$ is mostly 0, but it is 0.2% for $s = 10^2$. This shows a possibility for SIM to miss eigenvalues. In comparison, the results from NEW have all the ratios $\mathscr{R}_- = 0$. $\mathscr{R}_0$ is mostly 1 except for few larger s sizes where $\mathscr{R}_0$ is near 1. Thus, NEW has a small chance of accepting larger intervals that have no eigenvalues. (A possible reason is that the quadrature approximation with the Krylov subspace information is not accurate enough.) On the other hand, such over-detection for larger s is not a real problem: when a large interval without eigenvalues is further refined, the indicator will eventually find that there is no eigenvalue inside the subintervals. This is consistent with the self-correction effect mentioned above.

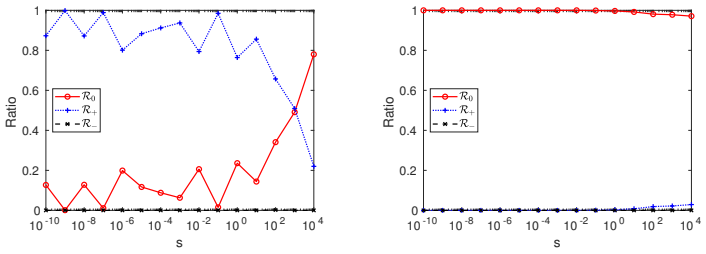

(a) SIM (b) NEW

Fig. 2 Example 1. Ratios $\mathscr{R}_0$, $\mathscr{R}_+$, and $\mathscr{R}_-$ for correct, over, and under detections, respectively, among 1000 randomly selected intervals of size s.

We also run another set of tests with different random z. The indicators are applied to an interval of length s randomly selected like above. This is done in $M = 1000$ runs, each with a different random z. Then we report the ratios $\mathscr{R}_0$, $\mathscr{R}_+$, and $\mathscr{R}_-$ (among M runs for each s) like the above in Figure 3. With SIM, the ratios are impacted by the choice of the random intervals, and there is a high percentage of over-detection for most of the s sizes. For $s = 10^4$, it further has $\mathscr{R}_- = 2.4\%$, again showing the possibility of falsely rejecting intervals. In comparison, with NEW, we have $\mathscr{R}_0 = 1$, $\mathscr{R}_+ = \mathscr{R}_- = 0$ consistently for all the s sizes. This confirms the high reliability of NEW for detecting eigenvalue existence.

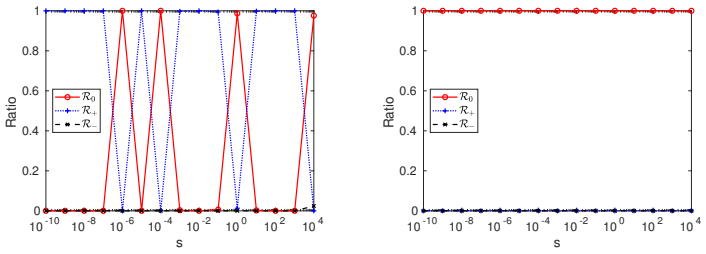

(a) SIM (b) NEW

Fig. 3 Example 1. Ratios $\mathscr{R}_0$, $\mathscr{R}_+$, and $\mathscr{R}_-$ for correct, over, and under detections, respectively, among 1000 runs each with a different random vector z.

As a particular example, we consider the interval $(10000, 10009)$ with one eigenvalue $\lambda = 10005.38603500869$ inside. We apply bisection and try to accurately locate λ through eigenvalue detection. With $\tau = 10^{-6}$, NEW uses $N_{\text{Kr}} = 1$ Krylov subspace to identify the eigenvalues as 10005.38603475690, which has absolute error $E = 2.52e-7 < \tau$. The corresponding residual is $\gamma = 6.24e-9$. On the other hand, SIM with $\delta = 0.05$ (and also $N_{\text{Kr}} = 1$) returns 139 eigenvalues, including some far away from the true eigenvalue. In fact, the largest distance between these eigenvalues from the true one is $2.83e-4$. SIM with $\delta = 0.4$ still returns two eigenvalues, including a spurious one.

Specifically, we can take a look at the subinterval $[10005.062500, 10005.343750]$ to see the self-correction effect of NEW. There is no eigenvalue in the interval. Since ξ_R in (8) is evaluated to be $1.03e-14$ which is just slightly larger than $\varepsilon = 10^{-15}$, this subinterval tentatively passes the safe rejection indicator and is not rejected. Then the interval is

bisected into the following two subintervals, where the corresponding ξ_R results are also given:

$$[10005.062500, 10005.203125], \quad \xi_R = 6.1472e-33,$$
$$[10005.203125, 10005.343750], \quad \xi_R = 1.7101e-20.$$

Both subintervals are then rejected by the safe rejection indicator with high confidence, correctly suggesting there is no eigenvalue in their parent subinterval.

Example 2 Next, consider the symmetric matrix A from `lowThrust_3` in the SuiteSparse sparse matrix collection [34]. A has size $n = 7064$ and $80,645$ nonzero entries. The results from eig are treated as the true eigenvalues λ_i. The matrix has some small eigenvalues clustered around 0.004515.

We first test randomly selected intervals and randomly selected vectors z like in Example 1. See Figures 4 and 5. We can draw conclusions similar to those in Example 1. With SIM, the $\mathscr{R}_-$ values in Figure 4(a) are 0.1%, 0.1%, and 0.5% for $s = 10^{-3}$, 1, and 10, respectively. This also indicates the chances for SIM to miss eigenvalues. NEW show significantly better reliability in Figures 4(b) and 5(b). In particular, the $\mathscr{R}_-$ ratios are all 0.

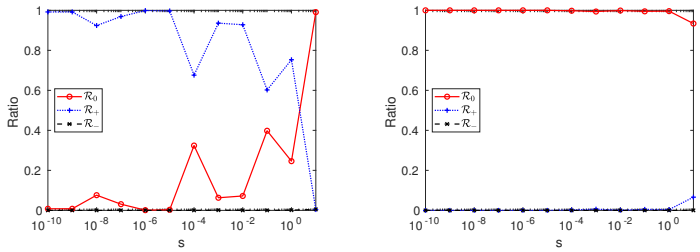

(a) SIM (b) NEW

Fig. 4 Example 2. Ratios $\mathscr{R}_0$, $\mathscr{R}_+$, and $\mathscr{R}_-$ for correct, over, and under detections, respectively, among 1000 randomly selected intervals of size s.

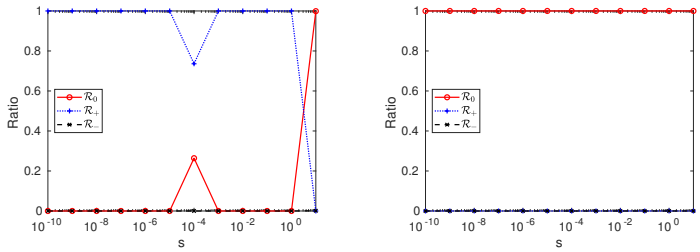

(a) SIM (b) NEW

Fig. 5 Example 2. Ratios $\mathscr{R}_0$, $\mathscr{R}_+$, and $\mathscr{R}_-$ for correct, over, and under detections, respectively, among 1000 runs each with a different random vector z.

Next, we try to accurately identify the smallest 20 eigenvalues of A, which are located within $(-0.004, 0.00451518)$. Most of them are highly clustered. Both NEW and SIM use $d = 30$, $N_{\mathrm{Kr}} = 20$, and $\tau = 10^{-10}$. Some eigenvalue results are given in Figure 6. Despite the eigenvalue clustering, NEW finds all the eigenvalues within the interval with $E = 4.53e-11$, $\gamma = 8.86e-10$. On the other hand, SIM returns some spurious eigenvalues with δ as small as 0.05 or as large as 0.4. If we further increase δ to 0.6, then SIM fails to identify any eigenvalue.

It is worth pointing out that, if the Matlab built-in function eigs is used to find these smallest eigenvalues (with the command eigs(A,20,'sm')), it is only able to find the 4 smallest ones that are not clustered. For the 16 eigenvalues near 0.004515, eigs fails to converge and outputs NaN (not-a-number). We may try to supply a shift to eigs. With the shift equal to 0.001, 0.002, or 0.003, eigs is only able to find no more than 3 eigenvalues and also takes longer. With the shift equal to 0.004, eigs misses the four smallest eigenvalues.

Example 3 Then consider a symmetric generalized eigenvalue problem $Aq = \lambda Bq$, where A and B are matrices related to localized quantum states in disordered media [3]. A and B have sizes $n = 61,440$ and each has $307,200$ nonzero entries. The Matlab function eigs are used to get λ_i.

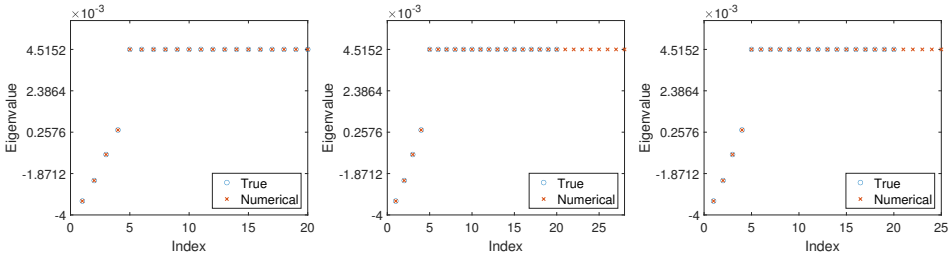

(a) $\tilde{\lambda}_i$ from NEW (b) $\tilde{\lambda}_i$ from SIM with $\delta = 0.05$ (c) $\tilde{\lambda}_i$ from SIM with $\delta = 0.4$

Fig. 6 Example 2. Numerical eigenvalues ($\times$) $\tilde{\lambda}_i$ within $(-0.004, 0.00451518)$ from NEW and SIM.

We first find the eigenvalues inside $(0.65, 0.85)$, which contains the 7 smallest eigenvalues of the problem. Both NEW and SIM use $d = 40$, $N_{\text{Kr}} = 2$, and $\tau = 10^{-8}$. See Table 2 for the eigenvalue results. NEW finds all the 7 eigenvalues with accuracy $E = 4.31e-09$, $\gamma = 8.40e-11$. Also, if we vary ε in NEW as $\varepsilon = 10^{-16}, 10^{-14}, \ldots, 10^{-8}$, similar accuracy results can be observed. SIM with $\delta = 0.05$ returns 9 eigenvalues, including two spurious ones. SIM with $\delta = 0.4$ does return exactly 7 eigenvalues satisfying the desired accuracy. However, if $\delta = 0.6$ is used, then SIM misses one eigenvalue that is in the subinterval $(0.835816192626953, 0.835816383361816)$. In fact, SIM outputs an estimate 0.501. Thus, a threshold larger than this would miss the eigenvalue. This shows that δ in SIM needs to be carefully tuned for this test. A similar behavior of SIM can be observed in the next example. In contrast, NEW uses the acceptance indicator in (10) based on the numerical estimate $\xi_N^{(2)} = 7.678e7$ to safely deduce the existence of eigenvalues inside. (Note this subinterval has a very small size so the quadrature points are very close to the target eigenvalue. The numerical approximation of the contour integral has a large norm unless a large number of quadrature points is used. For the purpose of eigenvalue detection, such large norms are not a problem.)

Table 2 Example 3. Eigenvalues within $(0.65, 0.85)$ from eigs, NEW, and SIM.

True (eigs)	NEW	SIM ($\delta = 0.05$)	SIM ($\delta = 0.6$)
0.669387778571829	0.669387778639793	0.669387778639793	0.669387778639793
0.714425860505378	0.714425858855247	0.669387791090374	0.714425858855247
0.807387579814707	0.807387575507164	0.714425858855247	0.807387581467629
0.835816383336921	0.835816380381584	0.714425871305828	0.836763045191765
0.836763044251227	0.836763045191765	0.807387581467629	0.845436832308769
0.845436833406130	0.845436832308769	0.835816380381584	0.848326924443245
0.848326926654481	0.848326924443245	0.836763045191765	
		0.845436832308769	
		0.848326924443245	

To demonstrate the robustness, we also run the methods with different parameters. With $\eta = 0.05, 0.1, 0.2, 0.4, 0.8$ and the other parameters the same as above, NEW finds all the 7 eigenvalues in $(0.65, 0.85)$ with consistent accuracy $E = 4.31e-09$, $\gamma = 8.40e-11$. Now with $\varepsilon = 10^{-16}, 10^{-14}, 10^{-12}, 10^{-10}, 10^{-8}$ and the other parameters the same as those at the beginning of the example, NEW finds all the 7 eigenvalues with accuracy given in Table 3. For larger ε, the number of subintervals visited is smaller so the cost is slightly lower. (The dominant cost is still for generating the Krylov subspaces. Here, the number of Krylov subspaces is $N_{\text{Kr}} = 2$ with all these ε.)

Table 3 Example 3. Accuracy of NEW with different rejection tolerances ε.

ε	10^{-16}	10^{-14}	10^{-12}	10^{-10}	10^{-8}
E	$5.02e-09$	$4.31e-09$	$4.31e-09$	$2.96e-09$	$2.95e-09$
γ	$8.40e-11$	$8.40e-11$	$8.40e-11$	$8.40e-11$	$8.40e-11$

Example 4 Now, consider a symmetric generalized eigenvalue problem $Aq = \lambda Bq$ related to a spectral method for the adversarial robustness evaluation of machine learning models [8]. A and B have sizes $n = 55,000$. A has $872,268$ nonzeros and B has $845,042$ nonzeros. The Matlab function eigs are used to get λ_i.

We look at the interval $(0,0.01)$, which contains 8 smallest eigenvalues of the problem. NEW and SIM both use $d=40$, $N_{\rm Kr}=1$, and $\tau=10^{-8}$. NEW finds 8 eigenvalues as follows with accuracy $E=2.94e-09$, $\gamma=3.46e-7$:

$$0.000000033378601,\ 0.003730750083923,\ 0.005356345176697,\ 0.006064696311951$$
$$0.006775670051575,\ 0.007296595573425,\ 0.009292960166931,\ 0.009675469398499$$

SIM with either $\delta=0.05$ or 0.4 returns 9 eigenvalues, including an spurious one. In particular, within the subinterval $(0.009675479398499, 0.009675483703613)$, the SIM estimator returns 0.515. Thus, a threshold smaller than this would return a spurious eigenvalue 0.009675481551056. In comparison, the safe rejection estimator of NEW is based on the estimate $\xi_R=2.119e-31$, which gives a solid indication that there is no eigenvalue inside.

Now, further increasing δ to 0.6 makes SIM fail to find any eigenvalue within the entire interval. In fact, the SIM estimator applied to $(0,0.01)$ returns the value about 0.5. Thus, any δ larger than this would fail. In contrast, NEW decides the existence of eigenvalues within the interval based on the numerical estimate $\xi_N^{(2)}=1.55e4$.

Finally, we test NEW with different accuracy control τ (and with the other parameters unchanged). Suppose $B=R^TR$ is the Cholesky factorization of the symmetric positive definite matrix B. Let $\tilde{\mathbf{q}}_i=R\tilde{q}_i/\|R\tilde{q}_i\|_2$ and $\tilde{\mathbf{Q}}$ be the matrix formed by all $\tilde{\mathbf{q}}_i$ corresponding to those eigenvalues in the interval $(0,0.01)$. Following [27], we let $\psi=\max_i \frac{\|\tilde{\mathbf{Q}}^T\tilde{\mathbf{q}}_i-\mathbf{e}_i\|_2}{\sqrt{n}}$ be the measurement of the loss of orthogonality, where $\mathbf{e}_i$ is the i-th unit vector. Table 4 shows the error, residual, loss of orthogonality, and timing with τ ranging from 10^{-4} to 10^{-14}. With τ reduces, the accuracy improves. With the different τ values, NEW has similar timing around 58 seconds. (In comparison, eigs takes 85.2 seconds).

Table 4 Example 4. Error, residual, and loss of orthogonality of NEW (with different τ).

τ	10^{-4}	10^{-6}	10^{-8}	10^{-10}	10^{-12}	10^{-14}
$N_{\rm bis}$	79	220	339	469	615	747
E	$3.90e{-5}$	$2.70e{-7}$	$2.94e{-9}$	$2.32e{-11}$	$3.64e{-13}$	$3.20e{-14}$
γ	$6.38e{-3}$	$4.43e{-5}$	$3.46e{-7}$	$3.79e{-09}$	$6.47e{-11}$	$1.15e{-12}$
ψ	$3.04e{-4}$	$2.90e{-6}$	$3.43e{-8}$	$2.56e{-10}$	$4.94e{-12}$	$8.32e{-14}$

Example 5 Lastly, consider a special example

$$A=\mathrm{diag}(-200,-199,\ldots,-10,0.1,0.2,\ldots,\underbrace{0.5,\ldots,0.5}_{\text{multiplicity 10}},0.6,\ldots,0.9,10,11,\ldots,200).$$

The matrix is diagonal so that it is known exactly to have 10 repeated eigenvalues $\lambda=0.5$. The matrix size is $n=400$.

We seek the 9 eigenvalues $0.1,0.2,\ldots,0.9$ within $(0,1)$. Note that if this interval is directly used as the initial search interval, its center c happens to be the eigenvalue $\lambda=0.5$ so that the algorithm would fail during the construction of the preconditioner in (15). This is similar to eigs which also fails if 0.5 is used as a shift. To avoid this, we may either add a small perturbation to $(0,1)$ similar to the suggestion from eigs documents or we may use a different interval.

Here, we try the initial search interval $[0.1,1]$. Note that now the eigenvalue $\lambda=0.1$ falls on the boundary. NEW with $d=20$, $N_{\rm Kr}=2$, and $\tau=10^{-10}$ properly identifies the 9 eigenvalues, including $\lambda=0.1$ on the boundary. The accuracy is $E=3.78e-11$, $\gamma=4.26e-11$.

As mentioned in Section 3.2, the multiple eigenvalue $\lambda=0.5$ is returned as a single eigenvalue. In order to identify its multiplicity, we may use the following strategy mentioned in [46]. Run the test with $\tilde{m}$ independent choices of random vector z in (13) and check the (numerical) linear independence of the outcome numerical eigenvectors $\tilde{q}$. That is, collect all $\tilde{q}$ into an $n\times\tilde{m}$ matrix $\tilde{Q}$ and compute the $\tilde{m}$ singular values σ_i of $\tilde{Q}$. If there are $\hat{m}(<\tilde{m})$ dominant singular values and the remaining ones are near 0, then $\hat{m}$ is the multiplicity. For example, for $\tilde{m}=12$, the singular values σ_i of $\tilde{Q}$ corresponding to the eigenvalues $\lambda=0.5$ and 0.1 are plotted in Figure 7. Clearly, for $\lambda=0.5$, there are 10 dominant singular values, indicating that the 12 runs produce 10 (numerically) linearly independent eigenvectors. This in turn reflects the multiplicity $\hat{m}=10$. Not surprisingly, for the eigenvalue $\lambda=0.1$, there is only one (numerically) independent eigenvector, indicating that it is a simple eigenvalue.

5 Concluding remarks

Indicator methods provide an elegant way for detecting eigenvalue existence. They apply the contour integral operator P to a single random vector z so as to tell if there are eigenvalues inside a region. Here for symmetric matrices, we

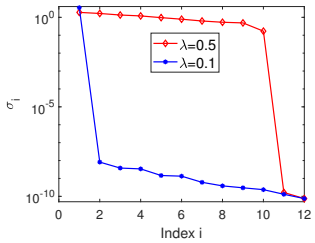

Fig. 7 Example 5. Singular values σ_i of the matrix $\tilde{Q}$ formed by the numerical eigenvectors (corresponding to λ) from 12 runs with independent z.

propose a strategy to overcome a major bottleneck of previous indicator methods in the threshold decision. That is, we give a robust way to decide the threshold based on rigorous statistical analysis of some estimators built upon Pz. We show that, if A has eigenvalues in an interval, the probability for some estimators to fail to indicate so is very small. Thus, we control the failure probability in our rejection indicator. We also use a framework to illustrate how our indicators may potentially be useful for finding eigenvalues and eigenvectors when they are combined with bisection and fast shifted linear system solution. The new indicators have significantly better robustness and reliability than those in [17–19], as demonstrated by extensive numerical tests.

The work in this paper provides new ways to use randomization for eigenvalue solutions. It also opens up more opportunities for subsequent studies such as the following topics.

- How to choose a low-accuracy quadrature rule that is fast and reliable enough for the purpose of eigenvalue detection instead of precise eigenvalue filtering?
- How to find an efficient and reliable preconditioner in the shifted linear system solution for the approximate indicator evaluation?
- How to tune the various parameters like the dimension of the Krylov subspace, the accuracy of the preconditioner, and the number of quadrature points so as to gain high efficiency without losing eigenvalues or producing spurious eigenvalues?

The indicator strategy can be readily modified for nonsymmetric matrices. The statistical analysis in Section 2.1 becomes more challenging. This will appear in our follow-up work [46].

Declarations

The data for the tests is available upon request. The authors declare that there is no conflict of interest.

References

1. M. Abramowitz and I. A. Stegun, Handbook of Mathematical Functions, Dover Publications, New York, 1965.
2. H. M. Aktulga, L. Lin, C. Haine, E. Ng, and C. Yang, Parallel eigenvalue calculation based on multiple shift-invert Lanczos and contour integral based spectral projection method, Parallel Comput., **40** (2014), pp. 195–212.
3. D. N. Arnold, G. David, D. Jerison, S. Mayboroda, and M. Filoche, Effective confining potential of quantum states in disordered media, Phys. Rev. Lett. 116 (2016), 056602.
4. A. P. Austin and L. N. Trefethen, Computing eigenvalues of real symmetric matrices with rational filters in real arithmetic, SIAM J. Sci. Comput., **37** (2015), pp. A1365–A1387.
5. H. Avron and S. Toledo, Randomized algorithms for estimating the trace of an implicit symmetric positive semi-definite matrix, J. ACM **58** (2011), Article 8.
6. O. Balabanov and L. Grigori, Randomized block Gram-Schmidt process for solution of linear systems and eigenvalue problems, (2021), arXiv:2111.14641.
7. Z. Bujanovic and D. Kressner, Norm and trace estimation with random rank-one vectors, SIAM J. Matrix Anal. Appl., **42** (2021), pp. 202–223.
8. W. Cheng, C. Deng, Z. Zhao, Y. Cai, Z. Zhang, and Z. Feng, SPADE: A spectral method for black-box adversarial robustness evaluation, (2021), arXiv:2102.03716.
9. J. D. Dixon, Estimating extremal eigenvalues and condition numbers of matrices, SIAM J. Numer. Anal., **20** (1983), pp. 812–814.
10. P. Drineas and M. Mahoney, RandNLA: Randomized Numerical Linear Algebra, Communications of the ACM, **59** (2016), pp. 80–90.
11. A. Frommer and U. Glässner, Restarted GMRES for shifted linear systems, SIAM J. Sci. Comput., **19** (1998), pp. 15–26.
12. W. Gautschi, Some elementary inequalities relating to the Gamma and incomplete Gamma function, J. Math. Phys., **38** (1959), pp. 77–81.
13. M. Gu, B. Parlett, D. Ting, and J. Xia, Low-rank update eigensolver for supercell band structure calculations, J. Comput. Electron., **1** (2002), pp. 411–414.

14. T. Gudmundsson, C. S. Kenney, and A. J. Laub, Small-sample statistical estimates for matrix norms, SIAM J. Matrix Anal. Appl., **16** (1995), pp. 776–792.
15. S. Güttel, E. Polizzi, P. Tang, and G. Viaud, Zolotarev quadrature rules and load balancing for the FEAST eigensolver, SIAM J. Sci. Comput., **37** (2015), pp. A2100–A2122.
16. N. Halko, P.G. Martinsson, and J. Tropp, Finding structure with randomness: Probabilistic algorithms for constructing approximate matrix decompositions, SIAM Review, **53** (2011), pp. 217–288.
17. R. Huang, A. Struthers, J. Sun, and R. Zhang, Recursive integral method for transmission eigenvalues, J. Comput. Phys., **327** (2016), pp. 830–840.
18. R. Huang, J. Sun, and C. Yang, Recursive integral method with Cayley transformation, Numer. Linear Algebra Appl., **25** (2018), e2199.
19. R. Huang, J. Sun and C. Yang, A multilevel spectral indicator method for eigenvalues of large non-Hermitian matrices, CSIAM Trans. Appl. Math., **1** (2020), 463–477.
20. V. Kalantzis, Y. Xi, and L. Horesh, Fast randomized non-Hermitian eigensolvers based on rational filtering and matrix partitioning, SIAM J. Sci. Comput., **43** (2021), pp. S791–S815.
21. C. S. Kenney and A. J. Laub, Small-sample statistical condition estimates for general matrix functions, SIAM J. Sci. Comput., **15** (1994), pp. 36–61.
22. B. Laurent and P. Massart, Adaptive estimation of a quadratic functional by model selection, Ann. Statist., **28** (2000), 1302–1338.
23. R. Li, Y. Xi, E. Vecharynski, C. Yang and Y. Saad, A Thick-Restart Lanczos algorithm with polynomial filtering for Hermitian eigenvalue problems, SIAM J. Sci. Comput., **38** (2016), pp. A2512–A2534.
24. P. G. Martinsson and J. Tropp, Randomized Numerical Linear Algebra: Foundations & Algorithms, Acta Numerica, (2020), arXiv 2002.01387.
25. R. A. Meyer, C. Musco, C. Musco, D. P. Woodruff, Hutch++: Optimal stochastic trace estimation, Symposium on Simplicity in Algorithms (SOSA), (2021), pp. 142–155.
26. Y. Nakatsukasa and J. A. Tropp, Fast & accurate randomized algorithms for linear systems and eigenvalue problems, (2021), arXiv:2111.00113.
27. X. Ou and J. Xia, SuperDC: Superfast divide-and-conquer eigenvalue decomposition with improved stability for rank-structured matrices, SIAM J. Sci. Comput., **44** (2022), pp. A3041–A3066.
28. B. N. Parlett, The Symmetric Eigenvalue Problem, Classics Appl. Math. 20, SIAM, 1998.
29. E. Polizzi, Density-matrix-based algorithm for solving eigenvalue problems, Phys. Rev. B, **79** (2009), 115112.
30. Y. Saad, Iterative Methods for Sparse Linear Systems, 2nd ed., SIAM, (2003).
31. Y. Saad, Numerical Methods for Large Eigenvalue Problems, 2nd ed., SIAM, (2011).
32. A. K. Saibaba, A. Alexanderian, and I. C. F. Ipsen, Randomized matrix-free trace and log-determinant estimators, Numer. Math., **137** (2017), pp 353–395.
33. T. Sakurai and H. Sugiura, A projection method for generalized eigenvalue problems using numerical integration, J. Comput. Appl. Math., **159** (2003), pp. 119–128.
34. SuiteSparse, http://faculty.cse.tamu.edu/davis/suitesparse.html.
35. K. M. Soodhalter, D. B. Szyld, and F. Xue, Krylov subspace recycling for sequences of shifted linear systems, Appl. Numer. Math., **81** (2014), pp. 105–118.
36. P. Tang and E. Polizzi, FEAST as a subspace iteration eigensolver accelerated by approximate spectral projection, SIAM J. Matrix Anal. Appl., **35** (2014), pp. 354–390.
37. L. N. Trefethen and J. A. C. Weideman, The exponentially convergent trapezoidal rule, SIAM Rev., **56** (2014), pp. 385–458.
38. J. A. Tropp, Randomized block Krylov methods for approximating extreme eigenvalues, Numer. Math., **150** (2022), pp. 217–255.
39. M. Van Barel, Designing rational filter functions for solving eigenvalue problems by contour integration, Linear Algebra Appl., **502** (2016), pp. 346–365.
40. J. G. Wendel, Note on the gamma function, Amer. Math. Monthly, **55** (1948), pp. 563–564.
41. J. D. Williams, An approximation to the probability integral, Ann. Math. Statist., **17** (1946), pp. 363–365.
42. F. Woolfe, E. Liberty, V. Rokhlin, and M. Tygert, A fast randomized algorithm for the approximation of matrices, Appl. Comput. Harmon. Anal., **25** (2008), pp. 335–366.
43. Y. Xi and Y. Saad, Computing partial spectra with least-squares rational filters, SIAM J. Sci. Comput., 38 (2016), pp. A3020–A3045.
44. Y. Xi, J. Xia, and R. Chan, A fast randomized eigensolver with structured LDL factorization update, SIAM J. Matrix Anal. Appl., **35** (2014), pp. 974-996.
45. J. Xia, Efficient structured multifrontal factorization for general large sparse matrices, SIAM J. Sci. Comput., **35** (2013), pp. A832–A860.
46. J. Xia and Q. Ye, Accurate randomized eigenvalue solution via the use of a single vector sample, preprint.
47. X. Ye, J. Xia, R. Chan, S. Cauley, and V. Balakrishnan, A fast contour-integral eigensolver for non-Hermitian matrices, SIAM J. Matrix Anal. Appl., **38** (2017), pp. 1268–1297.